


# Differential serotonergic modulation across the main and accessory olfactory bulbs

Zhenbo Huang<sup>1,3</sup>, Nicolas Thiebaud<sup>1,3</sup> and Debra Ann Fadool<sup>1,2,3</sup> 

<sup>1</sup>Program in Neuroscience, The Florida State University, Tallahassee, FL, USA

<sup>2</sup>Institute of Molecular Biophysics, The Florida State University, Tallahassee, FL, USA

<sup>3</sup>Department of Biological Science, The Florida State University, Tallahassee, FL, USA

## Key points

- There are serotonergic projections to both the main (MOB) and the accessory olfactory bulb (AOB).
- Current-clamp experiments demonstrate that serotonergic afferents are largely excitatory for mitral cells (MCs) in the MOB where 5-HT<sub>2A</sub> receptors mediate a direct excitatory action.
- Serotonergic afferents are predominately inhibitory for MCs in the AOB. There are two types of inhibition: indirect inhibition mediated through the 5-HT<sub>2</sub> receptors on GABAergic interneurons and direct inhibition via the 5-HT<sub>1</sub> receptors on MCs.
- Differential 5-HT neuromodulation of MCs across the MOB and AOB could contribute to select behaviours such as olfactory learning or aggression.

**Abstract** Mitral cells (MCs) contained in the main (MOB) and accessory (AOB) olfactory bulb have distinct intrinsic membrane properties but the extent of neuromodulation across the two systems has not been widely explored. Herein, we investigated a widely distributed CNS modulator, serotonin (5-HT), for its ability to modulate the biophysical properties of MCs across the MOB and AOB, using an *in vitro*, brain slice approach in postnatal 15–30 day mice. In the MOB, 5-HT elicited three types of responses in 93% of 180 cells tested. Cells were either directly excited (70%), inhibited (10%) or showed a mixed response (13%)—first inhibition followed by excitation. In the AOB, 82% of 148 cells were inhibited with 18% of cells showing no response. Albeit located in parallel partitions of the olfactory system, 5-HT largely elicited MC excitation in the MOB while it evoked two different kinetic rates of MC inhibition in the AOB. Using a combination of pharmacological agents, we found that the MC excitatory responses in the MOB were mediated by 5-HT<sub>2A</sub> receptors through a direct activation. In comparison, 5-HT-evoked inhibitory responses in the AOB arose due to a polysynaptic, slow-onset inhibition attributed to 5-HT<sub>2</sub> receptor activation exciting GABAergic interneurons. The second type of inhibition had a rapid onset as a result of direct inhibition mediated by the 5-HT<sub>1</sub> class of receptors. The distinct serotonergic modulation of MCs between the MOB and AOB could provide a molecular basis for differential chemosensory behaviours driven by the brainstem raphe nuclei into these parallel systems.

(Resubmitted 19 December 2016; accepted after revision 12 February 2017; first published online 22 February 2017)

**Corresponding author** D. A. Fadool: Florida State University, 319 Stadium Drive, King Life Sciences Building, Suite 3008, Tallahassee, FL 32306, USA. Email: dfadool@bio.fsu.edu

**Abbreviations** 5-HT, serotonin; ACSF, artificial cerebrospinal fluid; AOB, accessory olfactory bulb; AP, action potential; APV, D-(-)-2-amino-5-phosphonopentanoic acid; EPL, external plexiform layer; GC, granule cell; GCL, granule cell layer; IPI, interpulse interval; ISI, interspike interval; mAChR, muscarinic acetylcholine receptor; MC, mitral cell; MCL, mitral cell layer; MOB, main olfactory bulb; MOE, main olfactory epithelium; NBQX, 2,3-dihydroxy-6-nitro-7-sulfamoyl-benzo[f]quinoxaline; OB, olfactory bulb; OSN, olfactory sensory neuron; PG, periglomerular; RMP, resting membrane potential; SAC, short-axon cell; VNO, vomeronasal organ.

## Introduction

Monoamine 5-hydroxytryptamine (serotonin, 5-HT) is an important signalling molecule for a diverse number of behavioural and physiological functions (Berger *et al.* 2009), whereby at least 14 different 5-HT receptors have been identified and grouped into seven major subfamilies based upon structure, pharmacology and downstream signal transducing mechanism (Millan *et al.* 2008). In the CNS, serotonin and its various receptors regulate a breadth of neuropsychological processes including mood, reward, aggression, appetite and memory (Roth, 1994; Roth & Xia, 2004; Mittal *et al.* 2016). The CNS serotonin system mainly originates from the brainstem raphe nuclei and projects to almost every part of the brain (Jacobs & Azmitia, 1992). As such, all major brain areas express specific subfamilies of 5-HT receptors (Roth, 2007). Many receptor subfamilies are important therapeutic targets for anti-psychotic drug development and are of broad physiological importance for thermoregulation, pain, sleep and smooth muscle contraction (Reynolds *et al.* 2005; Pithadia & Jain, 2009; Palacios, 2016).

The olfactory bulb (OB) makes an amenable model to investigate serotonin neuromodulation due to its distinct anatomical organization that facilitates electrophysiological studies and its known receipt of serotonergic projections from the brainstem raphe nuclei (Broadwell & Jacobowitz, 1976; de Olmos *et al.* 1978; Araneda *et al.* 1980; McLean & Shipley, 1987; Suzuki *et al.* 2015). The OB is composed of two distinct structures: the main (MOB) and accessory olfactory bulb (AOB). Albeit sharing some common cytological organization with similarly named neurolamina – nomenclature that was carried forward from the MOB to the AOB by Ramon y Cajal (Figueres-Onate *et al.* 2014) – there are several noteworthy differences in the organization of AOB cell types whose biophysical analyses are largely incomplete. A prominent difference lies in the principal output neurons, called mitral cells (MCs), in both systems. In fact, Larriva-Sahd (2008) suggested that in the AOB, they should not actually be referenced as ‘mitral’ *per se* because their somata are not mitre in shape as they are in the MOB. AOB MCs are largely arranged as a scattered array, as opposed to a highly linear lamina, and have a multi-tufted morphology that terminates in 3–8 glomeruli rather than a single apical dendritic tuft leading to a single glomerulus (Ramon y Cajal, 1911; Takami & Graziadei, 1990; Jia *et al.* 1999; Urban & Castro, 2005). Hovis *et al.* (2012) examined the development of the unique circuit in the AOB to show that MC dendrites target glomeruli containing vomeronasal sensory neurons expressing the same receptor and that connectivity is both precise and activity modulated. As such, MOB and AOB MCs have distinct passive and active intrinsic properties to permit differential information processing (Zibman *et al.*

2011). Noguichi *et al.* (2014) support a computational model whereby dual informational processing might exist between the MOB and AOB. Shpak *et al.* (2012) and earlier *in vivo* work by Luo *et al.* (2003) demonstrate that AOB MCs, unlike those in the MOB, respond with strong, persistent excitation in response to transitory stimulation.

Despite initial explorations of basal biophysical differences across MOB and AOB MCs, the degree of neuromodulation across these systems has not been widely explored. One recent study has shown opposing effects of cholinergic modulation in the AOB *vs.* the MOB and suggests that these circuits utilize different physiological solutions for processing odour information (Smith *et al.* 2015). While there is strong structural and biophysical characterization of the role of serotonergic signalling in the MOB (Hardy *et al.* 2005; Petzold *et al.* 2009; Liu *et al.* 2012; Schmidt & Strowbridge, 2014; Suzuki *et al.* 2015; Brill *et al.* 2016), there are no biophysical studies in the AOB involving serotonin modulation despite anatomical evidence that suggests the existence of serotonergic fibres (Broadwell & Jacobowitz, 1976; Takeuchi *et al.* 1982). Early reports indicate the importance of serotonergic pathways in the regulation of innate behaviours such as aggression (Vergnes *et al.* 1974; Diuzhikova *et al.* 1987). Given the important roles of the accessory olfactory system in social and reproductive behaviours, serotonergic modulation of the AOB may be an important factor, but studies are needed to test this notion.

Given the diversity and widespread distribution of serotonin signalling in the CNS, noteworthy circuitry differences between the two partitions of the OB, differential expression of serotonin receptors across the MOB and AOB (McLean *et al.* 1995), and distinct firing properties of MCs across these structures, we undertook an exploration of serotonin neuromodulation using an *in vitro* slice preparation of the AOB *vs.* MOB. Utilizing a pharmacological approach across a large sampled population, 5-HT<sub>2A</sub> receptors appear to mediate a direct excitation of MOB MCs whereas two different serotonin receptor types appear to mediate an inhibition of AOB MCs. AOB MCs are indirectly inhibited through activation of GABAergic interneurons via 5-HT<sub>2</sub> receptors or are directly inhibited through 5-HT<sub>1</sub> receptors expressed on MCs. Economical utilization of the same molecule across two different parallel olfactory systems could serve to modulate distinct behaviours regulated by these olfactory sensory divisions.

## Methods

### Ethical approval

All animal experiments were approved by the Florida State University (FSU) Institutional Animal Care and

Use Committee (IACUC) under protocol no. 1427 and were conducted in accordance with the American Veterinary Medicine Association (AVMA) and the National Institutes of Health (NIH). In preparation for OB slice electrophysiology, mice were anaesthetized with isoflurane (Aerrane; Baxter, Deerfield, IL, USA) using the IACUC-approved drop method and were then killed by decapitation (AVMA Guidelines on Euthanasia, June 2007). All authors understood the ethical principles that *The Journal of Physiology* operates under and the work complied with the animal ethics checklist reported by Grundy (2015).

### Animal care

All mice (*Mus musculus*, C57BL/6J strain; The Jackson Laboratory, Bar Harbor, ME, USA) were housed at the FSU vivarium on a standard 12 h/12 h light/dark cycle and were allowed *ad libitum* access to 5001 Purina Chow (Purina, Richmond, VA, USA) and water. Mice of both sexes at postnatal day 15–30 were used for slice electrophysiology experiments, and had a body weight ranging from 5.7 to 17.5 g [mean (SD): 9.2 (3.5) g]. A total of 85 mice were used in the present study.

### Solutions and reagents

Artificial cerebral spinal fluid (ACSF) contained (in mM): 119 NaCl, 26.2 NaHCO<sub>3</sub>, 2.5 KCl, 1 NaH<sub>2</sub>PO<sub>4</sub>, 1.3 MgCl<sub>2</sub>, 2.5 CaCl<sub>2</sub>, 22 glucose; 305–310 mOsm.l<sup>-1</sup>, pH 7.3–7.4. Sucrose-modified ACSF (sucrose ACSF) contained (in mM): 83 NaCl, 26.2 NaHCO<sub>3</sub>, 1 NaH<sub>2</sub>PO<sub>4</sub>, 3.3 MgCl<sub>2</sub>, 0.5 CaCl<sub>2</sub>, 72 sucrose, 22 glucose; 315–325 mOsm.l<sup>-1</sup>, pH 7.3–7.4. The intracellular pipette solution contained (in mM): 135 potassium gluconate, 10 KCl, 10 Hepes, 10 MgCl<sub>2</sub>, 2 Na-ATP, 0.4 Na-GTP; 280–290 mOsm.l<sup>-1</sup>, pH 7.3–7.4. All salts and sugars were purchased from Sigma-Aldrich (St. Louis, MO, USA) or Fisher Scientific (Pittsburgh, PA, USA).

The synaptic blockers 2,3-dihydroxy-6-nitro-7-sulfamoyl-benzo[f]quinoxaline (NBQX), D-(-)-2-amino-5-phosphonopentanoic acid (APV) and 2-(3-carboxypropyl)-3-amino-6-(4 methoxyphenyl) pyridazinium bromide (gabazine) were purchased from Ascent Scientific (Princeton, NJ, USA). All synaptic blockers were prepared as stock solutions (NBQX 5 mM, APV 25 mM, gabazine 6 mM) in Milli-Q water and stored at –20°C. They were diluted to working concentrations (NBQX 5  $\mu$ M, APV 50  $\mu$ M, gabazine 6  $\mu$ M) in ACSF on the day of use.

The serotonin hydrochloride (5-HT) and serotonin receptor blockers methysergide maleate salt (methysergide), mianserin hydrochloride (mianserin), spiperone and pindolol were purchased from Sigma-Aldrich. Methysergide stock solution (2 mM)

was prepared in Milli-Q water and stored at –20°C. All other pharmacological agents were prepared at stock concentrations in ACSF (5-HT 0.8 mM, mianserin 80  $\mu$ M, spiperone 80  $\mu$ M, pindolol 2 mM with 1% acetic acid) and were diluted to working concentrations (5-HT typically 20, 40, 80  $\mu$ M, mianserin 20  $\mu$ M, spiperone 20  $\mu$ M, pindolol 20  $\mu$ M with 0.1% acetic acid) in ACSF on the day of use. Previous reports have used a working range of 20–50  $\mu$ M to explore 5-HT modulation in the MOB (Hardy *et al.* 2005; Brill *et al.* 2016). In our studies, 20  $\mu$ M 5-HT was used for MOB MC recordings whereas 40  $\mu$ M was used for AOB MC recordings. We elected to use a higher concentration in the AOB to accurately sample the modulation effect knowing there were fewer serotonergic projections to the AOB (Broadwell & Jacobowitz, 1976; Takeuchi *et al.* 1982). All pharmacological agents were introduced to OB slices through the bath chamber. Controls consisted of bath ACSF or vehicle control (ACSF plus 0.1% acetic acid) depending upon the pharmacological agent employed.

### OB slice electrophysiology

Mice were anaesthetized by inhalation of isoflurane (see Ethical approval) and quickly decapitated. The OBs were exposed by removing the dorsal and lateral portions of the skull between the lambda suture and the cribriform plate. The OBs were harvested and prepared for slice electrophysiology as described previously (Fadool *et al.* 2011). Briefly, after removing the dura, a portion of forebrain attached with the OBs was cut and quickly glued to a sectioning block with Superglue (Lowe's Home Improvement, USA), and submerged in oxygenated (95%O<sub>2</sub>/5%CO<sub>2</sub>), ice-cold, sucrose-modified ACSF for approximately 2 min prior to vibratome sectioning (Vibratome/Leica Model 1000, Wetzlar, Germany). Coronal sections were made at a thickness of 300  $\mu$ m and then allowed to recover in an interface chamber containing oxygenated ACSF (Krimmer & Goldman-Rakic, 1997) for 20–30 min at 33°C. The interface chamber was then maintained at room temperature (23°C) for about 60 min before recording. OB slices were recorded in a continuously perfused (Ismatec; 1–2 ml.min<sup>-1</sup>), submerged-slice recording chamber (RC-26, Warner Instruments, Hamden, CT, USA) with ACSF at room temperature. Slices were visualized at 10 $\times$  and 40 $\times$  using an Axioskop 2FS Plus microscope (Carl Zeiss Microimaging, Inc., Thornwood, NY, USA) equipped with infrared detection capability (Dage MTI, CCD100, Michigan, IN, USA). MCs in the MOB were identified as previously described (Fadool *et al.* 2011), while AOB lamination and MCs were identified based on previous reports (Salazar *et al.* 2001; Larriva-Sahd, 2008). Electrodes were fabricated from borosilicate glass (Hilgenberg no. 1405002, Malsfeld, Germany) to a pipette

resistance ranging from 4 to 7 M $\Omega$ . Positive pressure was retained while navigating through the OB laminae until a slight increase in the pipette resistance (typically 0.1–0.2 M $\Omega$ ) was observed, indicating that the pipette tip had made contact with the cell. A giga-ohm seal ( $R_e = 2.0$ –16.4 G $\Omega$ ) was achieved by releasing positive pressure and simultaneously applying a light suction. The whole-cell configuration was established by applying a rapid but strong suction to the lumen of the pipette while monitoring resistance.

After establishing a whole-cell configuration, MCs were first sampled for adequate resting potential (less than  $-55$  mV) and proper series resistance (less than 40 M $\Omega$ ) prior to initiating a series of current-clamp recordings. Perithreshold current levels were determined by incrementally injecting 1000-ms, 25-pA steps of current every 10 s, starting at  $-50$  pA. Following the determination of spike threshold, cells were then stimulated with a long, perithreshold current step of 5000 ms duration (typically ranging from 5 to 100 pA) every 10 s to acquire spike frequency data for MOB MCs. For some AOB MCs, an interpulse interval (IPI) of 10 s led to hyperpolarization of the cell. Thus, the IPI was increased to 18–22 s for some AOB MCs in order to adequately sample basal firing activity. The basal firing frequency was determined in control ACSF conditions for a minimum interval of 5 min by computing the mean firing frequency at the perithreshold step determined for an individual cell. The latency for the onset of suppression in AOB MCs was then measured as the time interval between the application of 5-HT and the time the firing frequency fell below this mean baseline frequency recorded for that cell. Because spike firing frequency was calculated across the duration of an applied current step (5 s) with a 10-s IPI, the resolution of the minimum onset latency for suppression was at least 15 s.

### Data acquisition and statistical analysis

Current-evoked changes in membrane voltage were measured using a Multiclamp 700B amplifier (Axon Instruments, Molecular Devices, Sunnyvale, CA, USA). The analog signal was filtered at 10 kHz and minimally digitally sampled every 100  $\mu$ s. The signals were digitized with a Digidata 1440A digitizer (Axon Instruments, Molecular Devices). The pipette capacitance was electrically compensated through the capacitance neutralization circuit of the Multiclamp 700B amplifier. Resting membrane potentials were corrected for a calculated  $-14$  mV junction potential offset. Membrane capacitance and input resistance were acquired from the membrane test function of Clampex 10.3 (Axon Instruments). Data were analysed using Clampfit 10.3 (Axon CNS), in combination with the analysis packages Origin 8.0 (MicroCal Software, Northampton, MA, USA)

and Igor Pro 6.0.2 (Wavemetrics Inc., Portland, OR, USA) with the NeuroMatics 2.02 plugin (written by Jason Rothman). MOB MCs usually exhibit an intermittent firing pattern and are characterized by variable spike clusters. A cluster was therefore defined as three or more consecutive spikes with an interspike interval (ISI) of 100 ms or less (Balu *et al.* 2004). Spike frequency (calculated throughout pulse depolarization), ISI (calculated within a spike cluster) and action potential cluster duration were measured as previously described (Balu *et al.* 2004; Fadool *et al.* 2011). Changes in the spike frequency were plotted as the mean percentage change compared to the control condition prior to bath application of the modulator. Baseline, treatment and washout values were calculated from the mean of at least 10 consecutive traces.

Statistical significance was determined between baseline biophysical property and that following the modulator using a two-tailed, paired *t* test or a one-way repeated measures ANOVA at the 95% confidence level ( $\alpha = 0.05$ ). Comparison of independent means was alternatively examined using a Student's *t* test. Spike firing frequency data were graphed by normalizing to the percent of the control condition, but non-normalized data were applied in the statistical analyses. All sampled populations were analysed using Prism 6 (GraphPad Software Inc., La Jolla, CA, USA). For all applied *t* tests and ANOVA tests, the assumptions of random sampling, normal distribution and equal variances were examined (Steel & Torre, 1980). Data were tested for equal variance using the Variance Ratio Test (two sample) or the Fmax test (ANOVA; variance within group) to ensure they did not violate the homogeneity of variance (Steel and Torre, 1980). Data were tested within the Prism software for normality using a D'Agostino–Pearson omnibus normality test. If any of the assumptions for a parametric design were violated or the sample size was small, corresponding non-parametric tests such as the Wilcoxon signed-rank test (non-parametric equivalent to paired *t* test) or Friedman test (non-parametric equivalent to repeated-measures ANOVA) were used. All reported values are mean (standard deviation, SD).

## Results

### Electrophysiological properties of MOB and AOB MCs

A total of 85 mice were used to acquire 328 recordings across our entire study for all electrophysiological measurements. Of the 180 MCs sampled from the MOB, 108 (60%) were spontaneously active; for AOB MCs, 70 out of 148 (47%) were spontaneously active under our recording conditions. For MOB MCs, more than half showed either spike clustering in spontaneously active neurons, or evoked spike clustering if they were initially



**Table 1. A comparison of intrinsic properties of MCs in the main olfactory bulb (MOB) versus the accessory olfactory bulb (AOB)**

	MOB	AOB
Membrane potential (mV)	−58.5 (3.3)	−67.6 (2.5)**
Membrane capacitance (pF)	117.1 (24.2)	84.3 (29.9)**
Input resistance (MΩ)	80.6 (21.7)	162.4 (67.2)**
Data are presented as mean (SD); $n = 24$ for MOB MCs, $n = 21$ for AOB MCs.		
**Significantly different mean values compared with MOB, Student's $t$ test, $P < 0.01$ .		

silent, but were activated by injecting current. Here, a cluster was defined as three or more consecutive spikes with an ISI of 100 ms or less (Balu *et al.* 2004). In contrast, sampled AOB MCs were rarely observed to have spike clusters. The intrinsic properties of our sampled MOB and AOB MCs are reported in Table 1. The membrane capacitance of MCs in the MOB was significantly greater than that in the AOB (Student's  $t$  test,  $P < 0.01$ ) while the input resistance was significantly less than that measured from the AOB (Student's  $t$  test,  $P < 0.01$ ). The mean resting membrane potential for MCs was more hyperpolarized in the AOB over that in the MOB (Student's  $t$  test,  $P < 0.01$ ). These distinct intrinsic properties of MOB and AOB MCs may reflect differences in the capacity for extrinsic modulation.

### The effects of 5-HT on MOB MCs

To study 5-HT modulation across the sampled MOB MC population, action potential (AP) threshold was initially determined using a brief current-step protocol (see Methods), and then cells were injected with the empirically defined perithreshold current (typically ranging from 5 to 100 pA) using a 5000 ms pulse duration every 10 s (IPI). Such spike firing frequency data were typically acquired for 30 min. A majority of the MOB MCs (126 of 180 examined; 70%) exhibited an increase in the evoked AP firing frequency in response to bath application of 5-HT (Fig. 1Aa). As shown in the comparative spike frequency plots, some cells (18/180; 10%) were inhibited by 5-HT (Fig. 1Ab). Another population of cells (23/180; 13%) exhibited a mixed response – first inhibition followed by excitation (Fig. 1Ac). A small proportion of the cells (13/180; 7%) did not respond to 5-HT. Because the majority of MCs were excited by 5-HT, we chose to only examine the biophysical details of this subtype of cells for the remainder of our study and did not explore inhibition or mixed-response cells. It was also possible to elicit increased AP firing frequency in cells held at rest without injected current in response to bath application of 5-HT (Fig. 1B). 5-HT bath application typically led to a small amplitude depolarization of 2.9 (1.6) mV after a delay of 18 (11) s [mean (SD),  $n = 15$ ]. The

depolarization was accompanied by an increased AP firing frequency. For both evoked and spontaneous activity, the latency to increase firing frequency in response to 5-HT was probably due to permeation time into the slice, rather than the time course for a transduction event. Unless specified otherwise, all our subsequent reported recordings were from evoked responses where spikes were quantified during the depolarizing pulse.

To systematically quantify the magnitude of the modulation by 5-HT, AP firing frequency of the evoked activity was averaged for 20 traces (5 min) in control ACSF solution (Fig. 2A, 'a'). Following bath introduction of 5-HT, the mean firing frequency was acquired for 20 traces (5 min) once the spike frequency was greater than the highest recorded value (in Hz) of the baseline, control activity (defined as an excitatory response) (Fig. 2A, 'b'). For washout measurements, AP firing frequency was determined, again for a mean of 20 traces once firing frequency reached original pre-modulation firing rates (Fig. 2A, 'c'). As shown in the bar graph of Fig. 2A, bath application of 5-HT resulted in a 6.8 (3.6)-fold ( $n = 15$ ) increase in firing frequency of MOB MCs over that of the control condition (significantly-different, one-way repeated-measures ANOVA,  $F_{2,28} = 166.4$ ,  $P < 0.0001$ , with Bonferroni's *post-hoc* test,  $P < 0.01$ ). In this, and subsequent repeated-measures ANOVA tests, the three treatment groups were control, modulator (5HT) and wash, yielding a degree of freedom of 2. The number of cells recorded across the three treatment groups is reported on the bar graphs, whereby the degree of freedom error was computed as degree of freedom within – degree of freedom subjects. The *post hoc* analyses sought the location of the variance between the treatment groups and is indicated by an asterisk at the given probability level ( $P$ ). MOB MCs usually exhibit an intermittent firing pattern that is characterized by variable-length spike clusters. 5-HT significantly increased the number of spike clusters recorded within a recording window of 10, 5000 ms traces [Fig. 2Bd; 15.4 (14.7) = Control vs. 53.2 (28.9) = 5-HT, significantly-different by paired  $t$  test,  $P < 0.01$ ,  $n = 17$ ] and increased the cluster duration [Fig. 2Be; 153.3 (80.6) ms = Control vs. 241.7 (124.8) ms = 5-HT, paired  $t$  test,  $P < 0.01$ ], but did not significantly change the ISI [Fig. 2Bf; 43.0 (9.7) ms = Control vs. 40.7 (8.7) ms = 5-HT, paired  $t$  test,  $P = 0.07$ ].

To determine if modulation altered AP shape in addition to firing frequency, similar within-cell recordings were made as in Fig. 2 but applying an increased sampling frequency (20 kHz) of the data to determine shape properties. As anticipated for a depolarized membrane, 5-HT significantly decreased the mean spike amplitude [68.9 (4.3) mV = Control; 67.1 (4.4) mV = 5-HT] while it increased AP half-width [1.4 (0.2) ms = Control; 1.5 (0.3) ms = 5-HT] and

10–90% rise time [0.7 (0.01) ms = Control; 0.8 (0.02) ms = 5-HT] (each significantly different by paired *t* tests,  $n = 15$ ,  $P < 0.01$ ). To examine whether 5-HT modulation depended upon synaptic processes or was intrinsic to MOB MCs, we tested for retention of 5-HT modulation for cells pre-incubated with fast glutamatergic and GABAergic synaptic blockers, namely a cocktail of NBQX, APV and gabazine. As shown in Fig. 3A, MOB MCs retained a strong increased firing frequency [7.8 (4.5)-fold increase] in response to 5-HT in the presence of synaptic blockers ( $n = 14$ ) that was significantly different (Fig. 3B; one-way repeated-measures ANOVA,  $F_{2,26} = 26.03$ ,  $P < 0.001$ , with Bonferroni's *post hoc* test,  $P < 0.01$ ). Although the excitatory effect of 5-HT in the presence of synaptic blockers (Fig. 3B) appeared larger than that in the absence of blockers (Fig. 2A), this differential did not reach statistical significance, suggesting that 5-HT modulation was not significantly influenced by additional circuits (Student's *t* test,  $n = 29$ ,  $P = 0.5211$ ). These collective data suggest that the excitatory effect of 5-HT on MOB MCs is probably direct or intrinsic, without the requirement of synaptic transmission.

### Pharmacological identification of serotonergic receptor type involved in the direct excitation of MOB MCs

Because our results indicated that 5-HT could directly depolarize the MOB MCs, we performed pharmacological tests to determine which 5-HT receptor might be involved in this action. For this series of pharmacological experiments, the non-selective 5-HT<sub>2,7</sub> receptor antagonist methysergide (Hoyer *et al.* 1994) was introduced into the bath following acquisition of firing frequency under control ACSF conditions (Fig. 4A). Subsequent co-presentation of 5-HT and methysergide failed to increase firing frequency in 6 of 6 cells tested [Fig. 4A, right, 0.4 (0.1) Hz = methysergide *vs.* 0.4 (0.3) Hz = methysergide plus 5-HT, not significantly different, paired *t* test,  $P > 0.05$ ]. Because a small percentage of MOB MCs were not excited by 5-HT, we completed a wash of the antagonist and then application of 5-HT to ensure the recorded neuron was indeed excitatory for the modulator (see Fig. 4A, left). Next, we tested mianserin, a more specific 5-HT<sub>2</sub> receptor antagonist (Hoyer *et al.* 1994). Here, MOB MCs were prescreened for 5-HT excitatory responses, washed and then pre-incubated

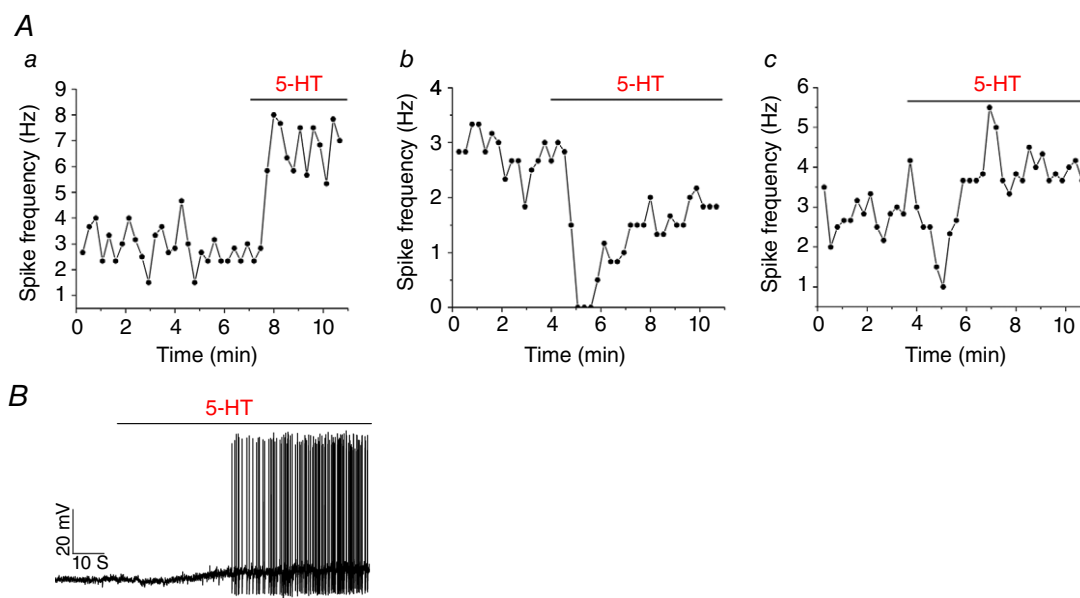


**Figure 1. Mitral cells in the main olfactory bulb (MOB MCs) largely exhibit an increase in action potential (AP) firing frequency in response to serotonin (5-HT)**

Aa–c, line graph summary of the changes in evoked, AP firing frequency in response to bath applied 5-HT indicated by the horizontal line for three representative MCs. Demonstrated is one representative cell from each type of response from the 180 cells sampled, where cells were: a, excited (126/180; 70%); b, inhibited (18/180; 10%); or c, demonstrated a mixed response to 5-HT (23/180; 13%) of first inhibition followed by excitation. A small portion of the cells (13/180; 7%) did not respond to 5-HT (*data not shown*). B, representative current-clamp recording of an MC at resting state in a whole-cell configuration. Bath application of 20  $\mu$ M 5-HT at the line; resting membrane potential = –62 mV. [Colour figure can be viewed at [wileyonlinelibrary.com](http://wileyonlinelibrary.com)]

with mianserin prior to co-presentation with mianserin and 5-HT (Fig. 4B, left). As shown in Fig. 4B, right, 5-HT excitation was also blocked by mianserin [1.0 (1.2) Hz = mianserin vs. 1.1 (1.5) Hz = mianserin plus 5-HT, not significantly different, Wilcoxon signed-rank test,  $P > 0.99$ ,  $n = 5$ ]. Spiperone, a more selective 5-HT<sub>2A</sub>

receptor antagonist (Hoyer *et al.* 1994), similarly prevented the excitatory effect of 5-HT in 7 of 8 cells tested using an identical protocol as that previously [Fig. 4C, 0.9 (0.7) Hz = spiperone vs. 0.5 (0.4) Hz = spiperone plus 5-HT, not significantly different, paired  $t$  test,  $P > 0.05$ ]. Finally, to confirm that the results of the receptor subtype

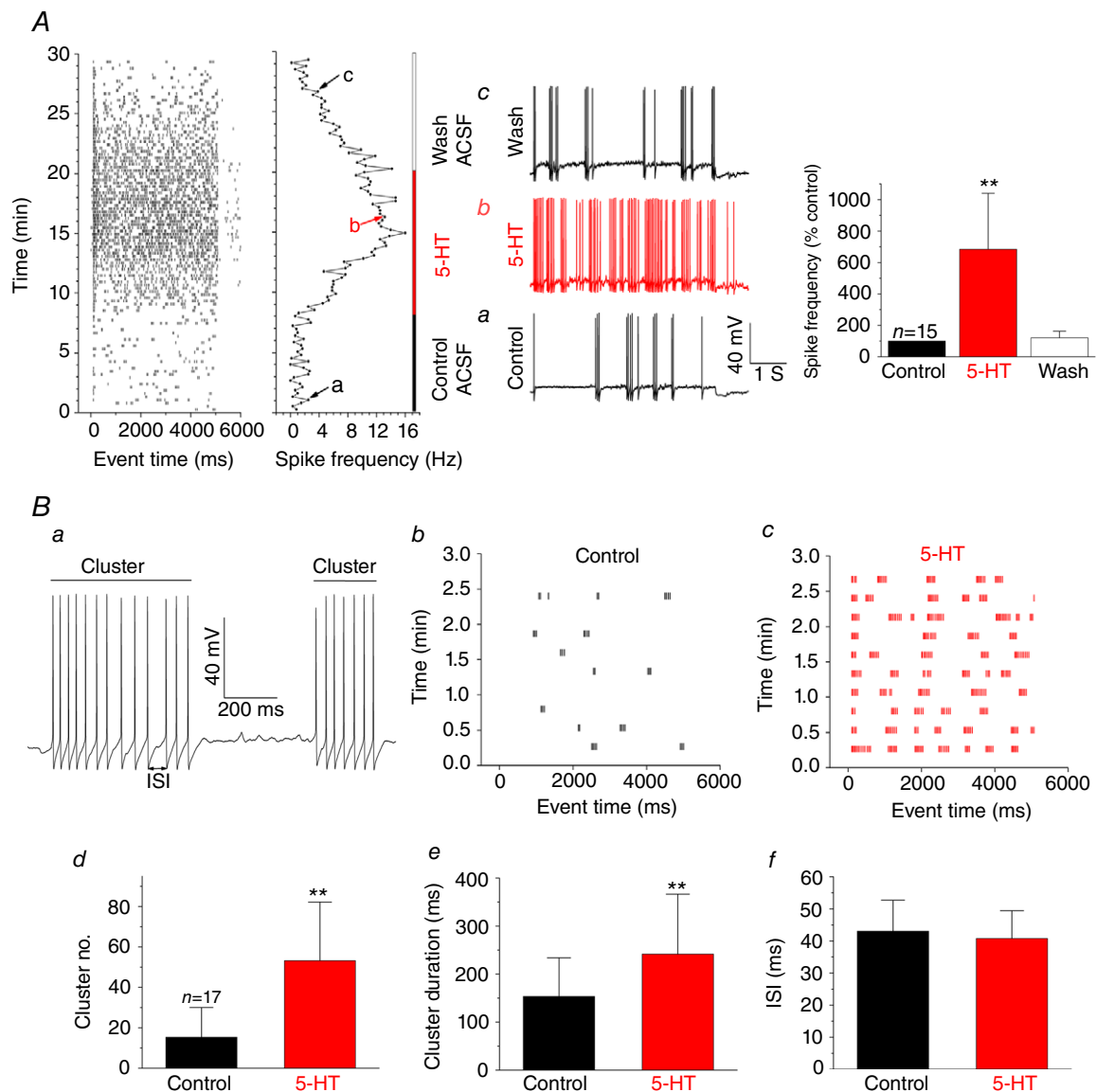


**Figure 2. Quantitative analysis of the excitatory response of MOB MCs**

A, left, raster plot showing evoked spike firing events binned in 5000 ms pulse duration (Event time) and recorded with an IPI of 10 s over a 25–30 min recording period, and the associated line graph of spike firing frequency under control ACSF, 5-HT and then wash ACSF conditions. Each vertical bar corresponds to the duration of the applied bath condition. Resting membrane potential =  $-64$  mV, 50 pA perithreshold current injection. Middle, representative current-clamp recordings for the cell on the left at time points a, b and c indicated at the arrows. Right, bar graph of a population of cells recorded as on the left ( $n = 15$ ). \*\*Significantly different from control, one-way repeated-measures ANOVA, Bonferroni's *post hoc* test,  $P < 0.01$ . B, spike cluster analysis. a, representative recording in control ACSF condition where two spike clusters (Cluster) and the inter-spike interval (ISI) are indicated. Raster plot collected for a cell as in A, under b, control ACSF and then c, 5-HT bath application. d–f, bar graphs indicating the mean number of AP clusters, cluster duration and ISI for a paired recording in control ACSF and then following 5-HT bath application. \*\*Significantly different from control, paired  $t$  test,  $n = 17$ ,  $P < 0.01$ . [Colour figure can be viewed at [wileyonlinelibrary.com](http://wileyonlinelibrary.com)]

pharmacology were the result of a direct effect on MCs, we extended these experiments to include the synaptic blockers, gabazine, NBQX and APV, as similarly applied in Fig. 3. In retesting cells for lack of serotonin excitation in the presence of the antagonists mianserin ( $n = 3$ ) and spiperone ( $n = 3$ ) using the synaptic blocker cocktail, both sets of experiments similarly prevented an increased firing frequency of MCs by 5-HT [ $0.2 (0.1) \text{ Hz} = \text{mianserin vs. } 0.2 (0.2) \text{ Hz} = \text{mianserin plus 5-HT}$ , not significantly different, Wilcoxon signed-rank test,  $P > 0.99$  and  $0.2 (0.01) \text{ Hz} = \text{spiperone vs. } 0.1 (0.01) \text{ Hz} = \text{spiperone plus 5-HT}$ , not significantly-different, Wilcoxon signed-rank test,  $P = 0.25$ ]. These collective data indicate that 5-HT direct modulation of MOB MCs occurs through a 5-HT<sub>2A</sub> receptor-mediated process.

### The effects of 5-HT on AOB MCs

In contrast to what was discovered for MOB MCs, the majority of AOB MCs (122/148; 82%) exhibited an inhibitory response to 5-HT rather than excitation (Fig. 5Aa,b). The remainder of the sampled AOB population (26/148; 18%) did not respond to 5-HT (Fig. 5Ac). In plotting a frequency distribution histogram for the onset times of all inhibitory responses (Fig. 5B), we found that there were two distinct populations, which we will refer to as slow-onset inhibition (as in Fig. 5Aa) and rapid-onset inhibition (as in Fig. 5Ab) types, respectively (significantly different means, Student's  $t$  test with Welch's correction,  $P < 0.0001$ ). Seventy-four out of 122 cells had onset times that fell within the Gaussian fit of the slow-onset inhibition type [mean (SD), 166 (47.3) s] in response to 5-HT modulation, while 48 out of

122 cells had much quicker onset times for inhibition by 5-HT [27 (4.8) s] and fell within the fit for the rapid-onset inhibition. Similar to that found with MOB MCs, spontaneous activity of AOB MCs could also be modulated by bath-applied 5-HT (Fig. 5C).

When we quantified the magnitude of the modulation by 5-HT systematically, we found there were two different magnitudes of inhibition, regardless of onset kinetics. The first was a weak inhibition, in which the spike frequency was modestly, but significantly, reduced by 5-HT compared with the control condition (Fig. 6A, Friedman's test,  $P = 0.0002$ , with Dunn's *post hoc* test,  $P < 0.01$ ,  $n = 9$ ). The second group exhibited strong inhibition to 5-HT. Here, 5-HT bath application gradually delayed the latency of the first evoked spike of the cell until it stopped firing compared with the control condition (Fig. 6B, Friedman's test,  $P < 0.0001$ , with Dunn's *post hoc* test,  $P < 0.01$ ,  $n = 9$ ). Correspondingly opposite to what we found for excitatory MOB MCs, the AP shape for AOB MCs exhibited an increase in peak amplitude [ $83.4 (7.0) \text{ mV} = \text{Control}$ ;  $86.3 (7.5) \text{ mV} = 5\text{-HT}$ ], a reduction in the half-width [ $2.6 (0.4) \text{ mV} = \text{Control}$ ;  $2.3 (0.4) \text{ mV} = 5\text{-HT}$ ] and 10–90% rise time [ $0.9 (0.1) \text{ mV} = \text{Control}$ ;  $0.8 (0.2) \text{ mV} = 5\text{-HT}$ ] (each significantly different, paired  $t$  test,  $P < 0.01$ ,  $n = 10$ ). These data were pooled from both weakly and strongly inhibited cells regardless of onset of modulation, because all types of inhibited AOB MCs demonstrated the same change in AP shape. To identify whether synaptic transmission was required for 5-HT inhibitory responses for either slow-onset inhibition or rapid-onset inhibition in AOB MCs, experiments were performed in the presence of gabazine (GABA<sub>A</sub> receptor antagonist) in ACSF. Two different types of responses

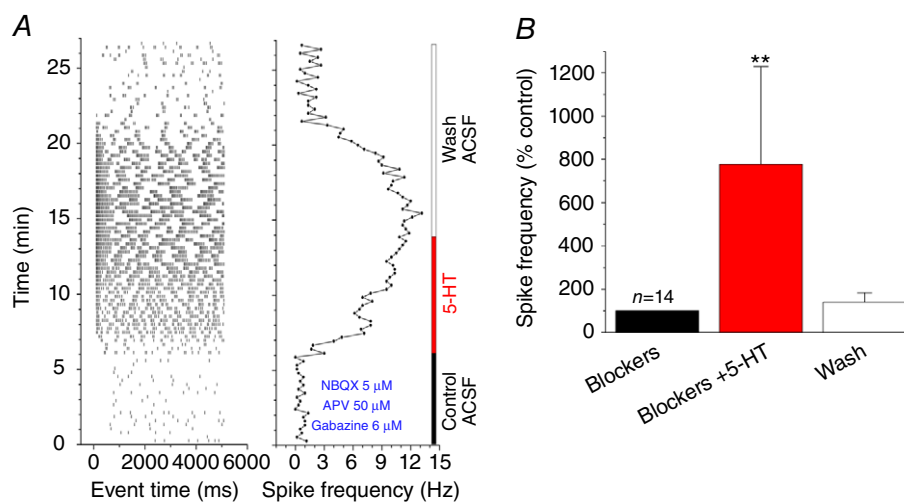


**Figure 3. 5-HT elicits direct excitation of MOB MCs**

A, raster plot as in Fig. 2 but where evoked responses were recorded in the presence of NBQX ( $5 \mu\text{M}$ ), APV ( $50 \mu\text{M}$ ) and gabazine ( $6 \mu\text{M}$ ). Resting membrane potential =  $-61 \text{ mV}$ ;  $75 \text{ pA}$  perithreshold current injection. B, bar graph of the mean spike frequency expressed as percent of the basal firing of the control. Same statistical analysis and notations as in Fig. 2A,  $n = 14$ . [Colour figure can be viewed at [wileyonlinelibrary.com](http://wileyonlinelibrary.com)]



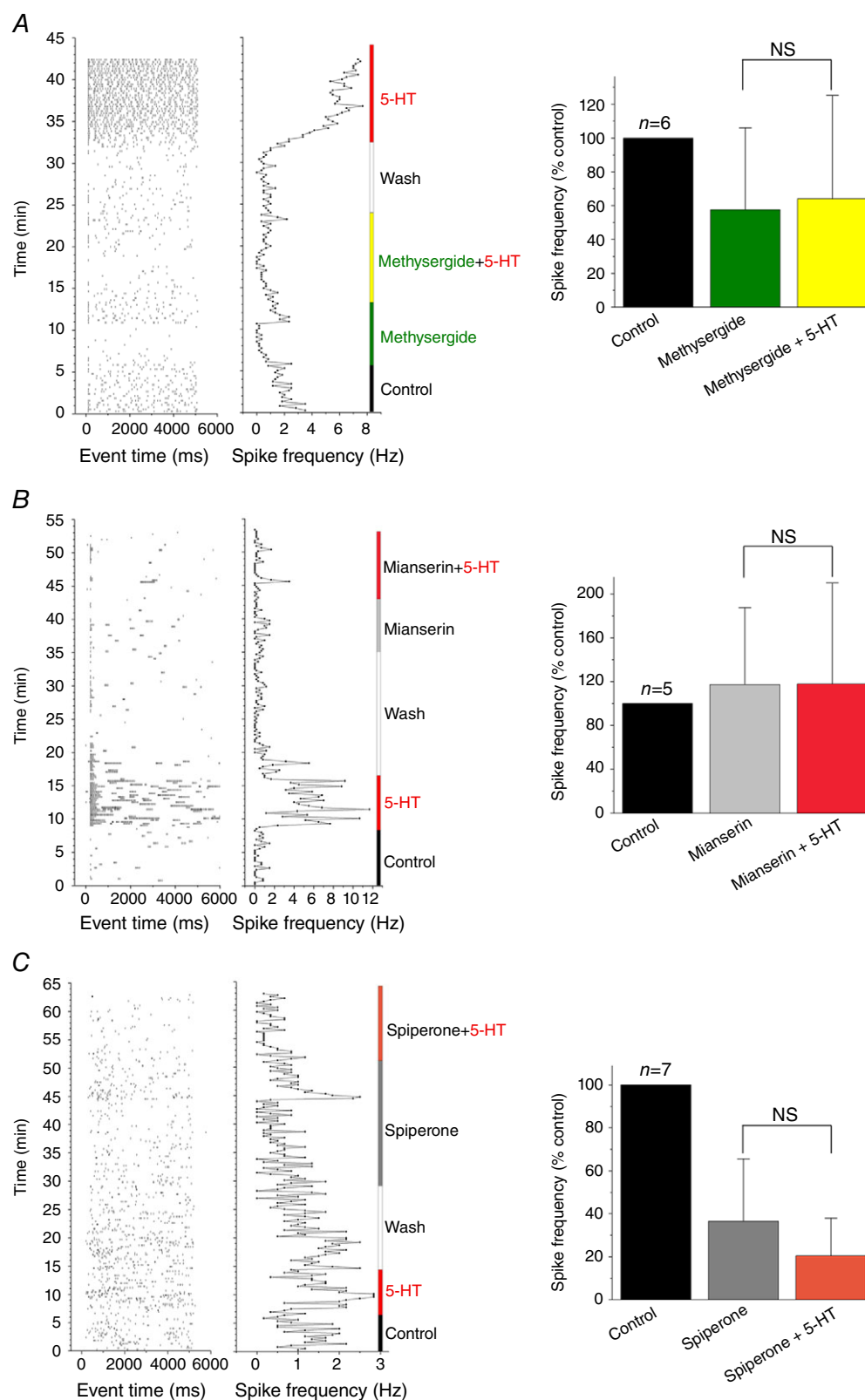


**Figure 4. 5-HT-evoked excitation in MOB MCs is inhibited by 5-HT receptor antagonists that have subtype specificity**

Representative raster plots and associated spike frequency line graphs acquired and constructed for evoked activity as in Fig. 2A. A, *left*, representative recording whereby the MC was preincubated with the non-selective 5-HT<sub>2,7</sub> receptor antagonist, methysergide, prior to co-presentation of the inhibitor plus 5-HT. Note that following a

wash, application of 5-HT confirmed the neuron was excited by the modulator. *Right*, bar graph of the mean spike frequency expressed as percent of the basal firing of the control for six such recordings. *B*, *left*, as in *A*, but applying the 5-HT<sub>2</sub> receptor antagonist mianserin. *Right*, bar graph of the mean spike frequency expressed as percent of the basal firing of the control for five such recordings. *C*, *left*, as in *A*, but applying a more selective 5-HT<sub>2A</sub> receptor antagonist, spiperone. *Right*, bar graph of the mean spike frequency expressed as percent of the basal firing of the control for seven such recordings. AC, NS = not significantly different, paired *t* test,  $P > 0.05$ . B, NS = not significantly different, Wilcoxin signed-rank test,  $P > 0.05$ . [Colour figure can be viewed at [wileyonlinelibrary.com](http://wileyonlinelibrary.com)]

were observed – slow-onset inhibition responding to gabazine application and rapid-onset inhibition that was insensitive to gabazine application. Five sampled cells that were found to be the slow-onset inhibition type failed to be modulated by 5-HT following gabazine pre-incubation. For these recordings (Fig. 7A), baseline AP firing frequency was first determined in control ACSF and then 5-HT was introduced to determine that the cell was slowly inhibited by the modulator. Gabazine was then introduced to the bath followed by a co-presentation of gabazine plus 5-HT. Finally, following wash out of both agents, 5-HT was re-applied to confirm continued inhibitory response to the modulator. As determined for the population of sampled AOB MCs, slow-onset inhibition appeared to be mediated by GABA transmission because adding gabazine prevented the inhibitory effect of 5-HT [Fig. 7A, 2.2

(1.0) Hz = gabazine *vs.* 2.3 (1.2) Hz = gabazine plus 5-HT, not significantly different, Wilcoxin signed-rank test,  $P > 0.81$ ,  $n = 5$ ]. To confirm that 5-HT in the AOB was exciting GABAergic neurons that could inhibit MCs via GABA release and not causing an excitation of glutamatergic neurons that could in turn excite GABAergic neurons to inhibit MCs, it was important to delineate between these alternatives by preventing synaptic transmission of glutamate. Therefore, in the presence of APV/NBQX, we report that 4 of 4 cells still exhibited slow-onset inhibition [Fig. 7B, 1.9 (0.6) Hz = APV/NBQX *vs.* 1.0 (0.6) Hz = APV/NBQX plus 5-HT, significantly different, Wilcoxin signed-rank test,  $P < 0.04$ ,  $n = 4$ ]. For these recordings (Fig. 7B), cells were first confirmed to be slowly inhibited by 5-HT and following a wash, 5-HT was reintroduced, but in the

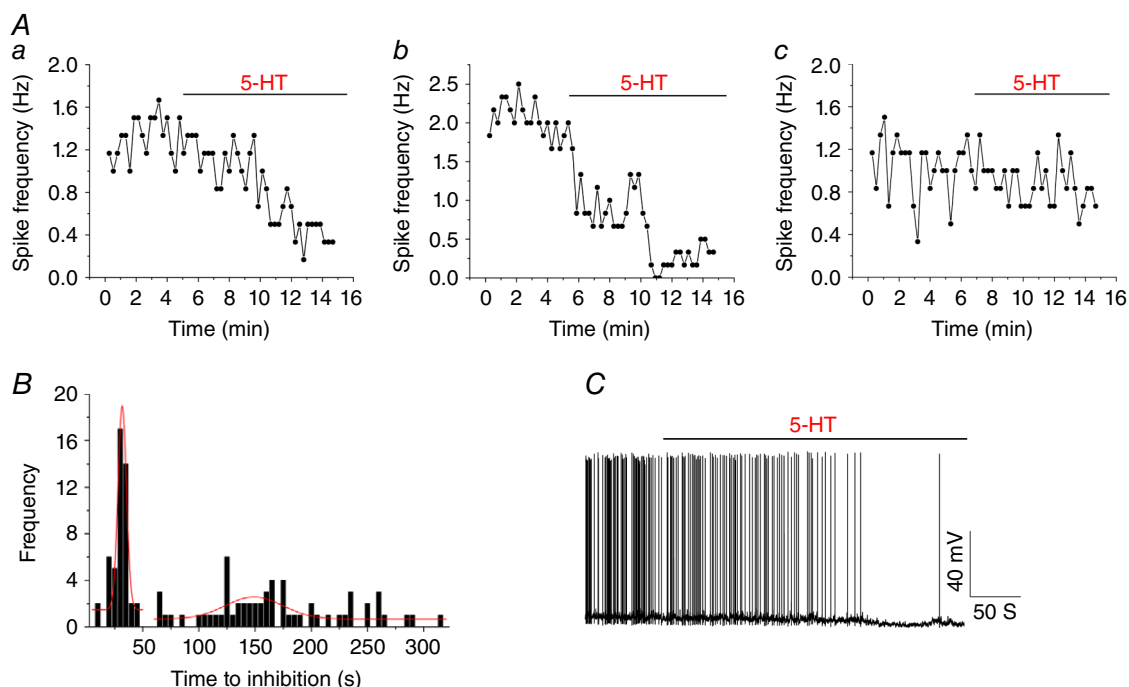


**Figure 5. Mitral cells in the accessory olfactory bulb (AOB MCs) predominantly exhibit a decrease in action potential (AP) firing frequency in response to serotonin (5-HT)**

Aa–c, line graph summary of the changes in evoked, AP firing frequency in response to bath-applied 5-HT indicated by the horizontal line for three representative MCs. Demonstrated is one representative cell from each type of response from the 148 cells sampled, where: a, slow-onset (74/148; 50%); or b, rapid-onset (48/148; 32%) inhibition was recorded. A population of cells (c, 26/148; 18%) did not respond to 5-HT. B, histogram distribution plot of the onset latency times for inhibition by 5-HT. Two separate distributions, a slow-onset inhibition (right Gaussian) and a rapid-onset inhibition (left Gaussian), were fit from the sampled population. C, representative current-clamp recording of a spontaneously active MC in whole-cell configuration. Bath application of 40  $\mu$ M 5-HT at the line; resting membrane potential =  $-65$  mV. [Colour figure can be viewed at [wileyonlinelibrary.com](http://wileyonlinelibrary.com)]

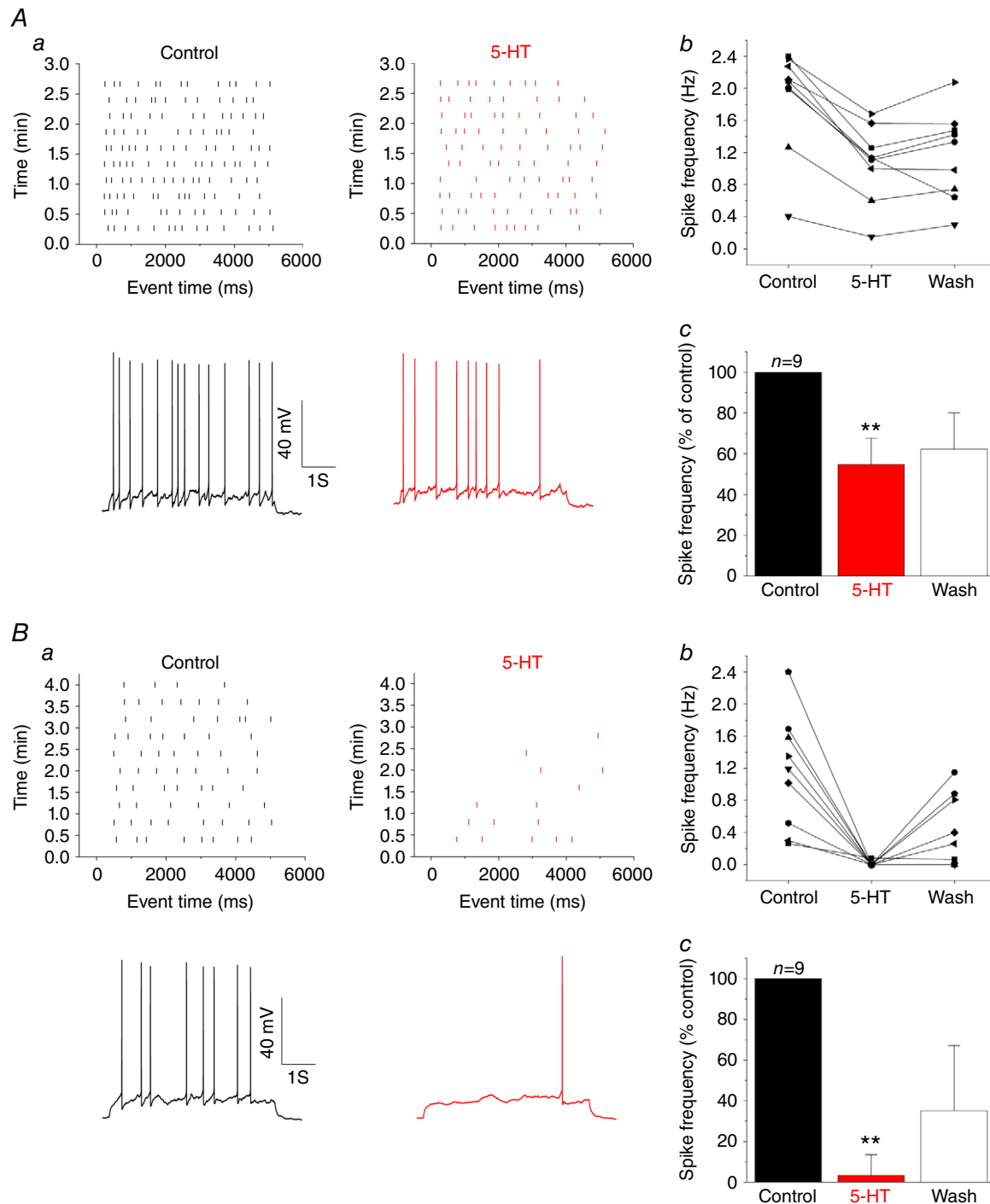


**Figure 6. AOB MCs are differentially inhibited by 5-HT, regardless of onset kinetics of the modulation**

Current-clamp recordings and associated raster plots for a representative MC that was Aa, weakly inhibited [resting membrane potential (RMP) =  $-67$  mV; 25 pA perithreshold current injection] vs. one that was Ba, strongly inhibited by 5-HT (RMP =  $-69$  mV; 30 pA perithreshold current injection). For cells responding to 5-HT with the latter type of inhibition, 5-HT progressively delayed the latency to first spike until the cell stopped firing in later trace numbers. AB, parts a, note that AP firing in AOB MCs does not exhibit cluster behaviour as demonstrated in the raster plots. AB, parts b, line graphs showing the spike frequencies for individual cells under the control, 5-HT and wash conditions. AB, parts c, bar graphs of the mean spike frequency expressed as percent of the basal firing of the control. \*\*Significantly different from control, Friedman's test, Dunn's *post hoc* test,  $P < 0.01$ . [Colour figure can be viewed at [wileyonlinelibrary.com](http://wileyonlinelibrary.com)]

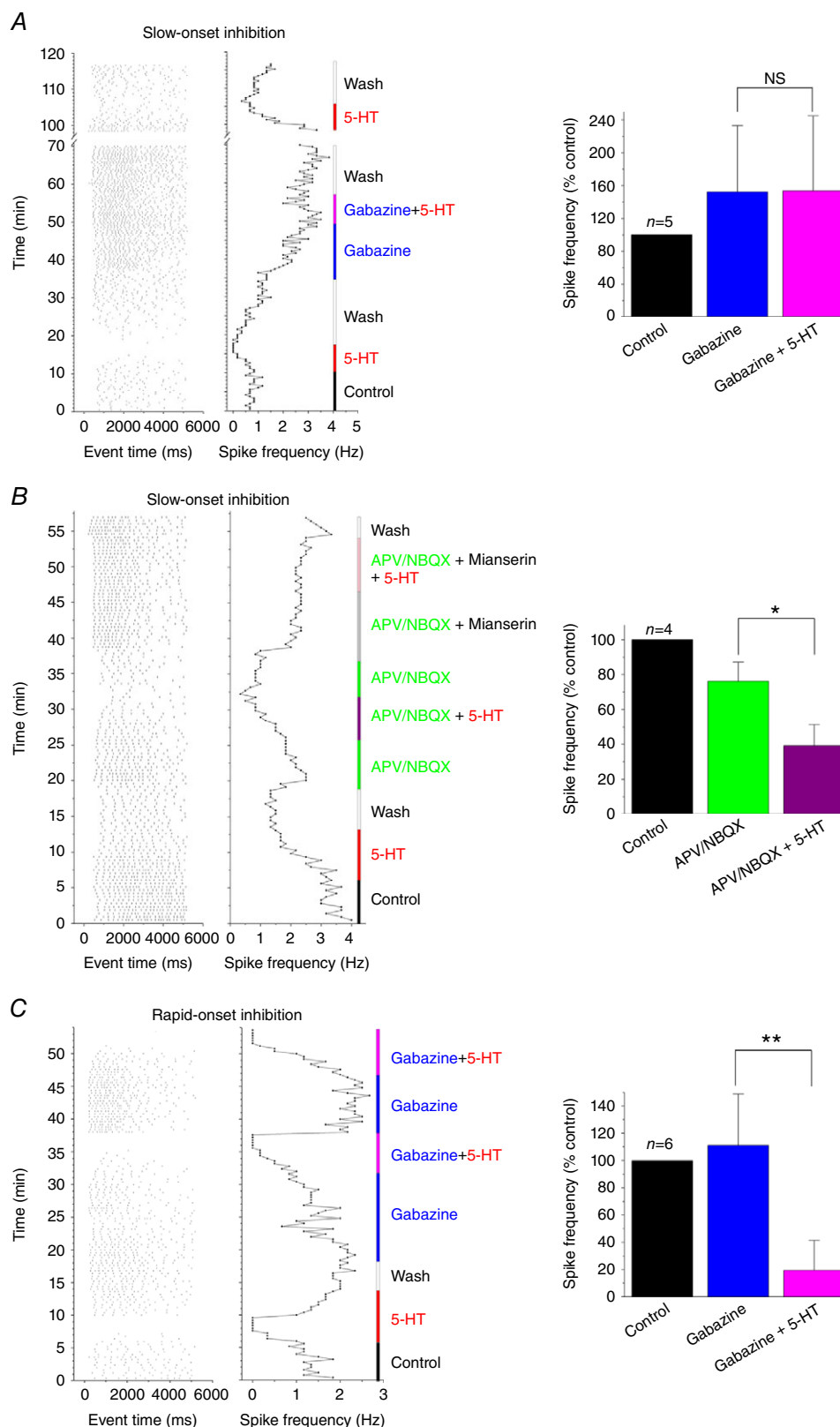


**Figure 7. 5-HT-evoked inhibition in AOB MCs responds differentially to gabazine**

Representative raster plot and spike frequency line graphs generated as in Fig. 3 for an MC that was inhibited by 5-HT with *AB* slow-onset vs. *C*, rapid-onset modulation. *A*, *left*, note that the slow-onset 5-HT modulation was



blocked by pre-incubation with gabazine after which co-presentation of gabazine plus 5-HT failed to inhibit firing frequency. This could be recovered following a wash (*time break bar*) and inhibited again via 5-HT application alone. *B, left*, note that the slow-onset 5-HT modulation was not blocked by pre-incubation and then co-presentation with synaptic blockers (APV/NBQX). Using a continual background of synaptic blockers, the 5-HT<sub>2</sub> receptor antagonist, mianserin, blocked the slow-onset inhibition. *C, left*, note that the rapid-onset 5-HT modulation was not blocked by pre-incubation with gabazine after which co-presentation of gabazine plus 5-HT continued to elicit rapid inhibition by 5-HT. This was repeatable within the same cell. *A–C, right*, bar graphs of the mean spike frequency expressed as percent of the basal firing of the control for both kinetic types of inhibitory responses. *A, right*, NS = not significantly different, Wilcoxin signed-rank test,  $n = 5$ ,  $P > 0.05$ . *B, right*, \*significantly different Wilcoxin signed-rank test,  $n = 4$ ,  $P < 0.04$ . *C, right*, \*\*significantly different, paired  $t$  test,  $n = 6$ ,  $P < 0.01$ . [Colour figure can be viewed at [wileyonlinelibrary.com](http://wileyonlinelibrary.com)]

presence of APV/NBQX (Fig. 7B). Among these four cells, we examined three with the 5-HT<sub>2</sub> receptor antagonist mianserin in the continued presence of APV/NBQX. Mianserin co-presented with 5-HT blocked the slow-onset inhibition [2.8 (0.8) Hz = APV/NBQX plus mianserin vs. 2.8 (0.9) Hz = APV/NBQX plus mianserin and 5-HT, Wilcoxin signed-rank test,  $P = 0.99$ ,  $n = 3$ ] (Fig. 7B). To our surprise, six sampled AOB MCs demonstrated that 5-HT rapid-onset inhibition could not be blocked by gabazine (Fig. 7C). Here, 5-HT was confirmed to rapidly inhibit evoked AP firing frequency, but when washed and pre-incubated with gabazine as in the first sampled population, co-presentation of gabazine and 5-HT continued to elicit an inhibition of firing frequency, like that of 5-HT alone [Fig. 7C, 1.3 (0.5) Hz = gabazine vs. 0.2 (0.2) Hz = gabazine plus 5-HT, significantly different, paired  $t$  test,  $P < 0.01$ ,  $n = 6$ ]. This was repeatable within the same cell. Additionally, following an extended wash of these agents, pre-incubation with the broad spectrum antagonist methysergide and then co-presentation of methysergide and 5-HT did prevent the inhibitory effect of 5-HT (data not shown). We therefore speculated that the rapid-onset inhibition could be a direct effect of 5-HT on MCs. To confirm our conjecture, we performed further pharmacological tests as described below.

### Pharmacological identification of receptor types involved in 5-HT actions on AOB MCs

Because our results suggested there were two types of 5-HT inhibition of AOB MCs – a slow-onset inhibition and rapid-onset inhibition – we hypothesized that the slower onset inhibition might use a polysynaptic mechanism. As such, 5-HT would be expected to initially excite GABAergic interneurons that, in turn, could release GABA onto MCs to inhibit their activity. We confirmed that the slow-onset inhibition could be blocked by the non-selective 5-HT<sub>2,7</sub> receptor antagonist methysergide [Fig. 8A, 1.0 (0.7) Hz = methysergide vs. 1.2 (0.8) Hz = methysergide plus 5-HT, not significantly different, Wilcoxin signed-rank test,  $P = 0.13$ ,  $n = 4$ ] and 5-HT<sub>2</sub> receptor antagonist mianserin [Fig. 8B, 1.3 (0.3) Hz = mianserin vs. 1.4 (0.4) Hz = mianserin plus 5-HT, not significantly different, Wilcoxin signed-rank test,

$P = 0.44$ ,  $n = 5$ ]. Here, 5-HT was first applied to confirm slow inhibition, followed by a wash and then application of the antagonist (noted as Methysergide-1 or Mianserin-1). Because the antagonist elicited strong inhibition, current injection was increased to elevate spike firing frequency (noted as Methysergide-2 or Mianserin-2) prior to co-presentation of 5-HT and the antagonist. Because mianserin prevented slow-onset inhibition (Figs 7B and 8B) but not rapid-onset inhibition (data not shown), this may suggest that the subtype of 5-HT receptors mediating the two kinetically distinct types of inhibition may be different. 5-HT<sub>1</sub> receptors, including 5-HT<sub>1A/B</sub>, have been shown to mediate both pre- and post-synaptic inhibitory effects of 5-HT (Blier *et al.* 1998; Morikawa *et al.* 2000; Ogren *et al.* 2008). We therefore examined whether the 5-HT<sub>1A/B</sub> receptor antagonist pindolol (Hoyer *et al.* 1994) could prevent the rapid-onset inhibition by 5-HT. As shown in Fig. 8C, the rapid-onset 5-HT inhibition that is independent of GABAergic transmission (not blocked by gabazine) could be blocked by pindolol in 4 of 5 tested cells [1.0 (0.1) Hz = pindolol vs. 1.1 (0.3) Hz = pindolol plus 5-HT, not significantly different, Wilcoxin signed-rank test,  $P = 0.38$ ]. Finally, block by pindolol in the presence of gabazine was additionally examined, which similarly demonstrated a block of the rapid-onset inhibition by 5-HT [1.1 (0.8) Hz = gabazine and pindolol vs. 1.0 (0.6) Hz = gabazine and pindolol plus 5-HT, not significantly different, Wilcoxin signed-rank test,  $P = 0.25$ ,  $n = 4$ ].

### Discussion

Despite the conserved circuitry of 5-HT arriving from centrifugal projections of the CNS (Devore & Linster, 2012; Smith *et al.* 2015), our electrophysiological results demonstrate striking differences in serotonergic modulation. 5-HT was predominantly excitatory for MCs of the MOB, although both inhibition and mixed excitation/inhibition were observed to a lesser frequency, while modulation was strictly inhibitory for those in the AOB. AOB inhibitory responses were classified by two different kinetic rates of inhibition – slow-onset inhibition and rapid-onset inhibition, respectively – and were found to be governed by two different subfamilies of 5-HT receptors. The diversity of responses to 5-HT in the MOB

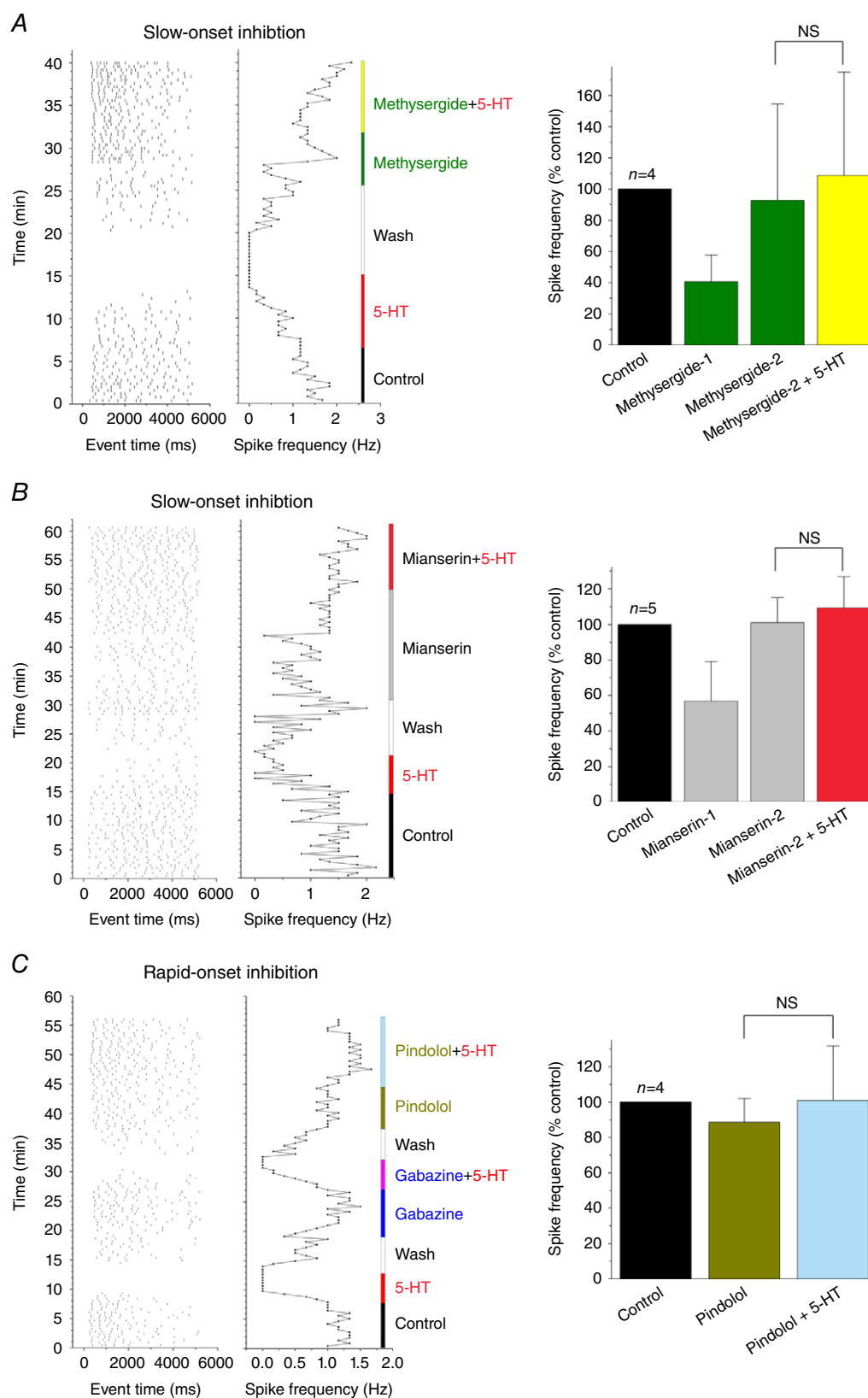


**Figure 8. Slow-onset 5-HT modulation is sensitive to 5-HT<sub>2</sub> receptor antagonists while rapid-onset modulation is sensitive to 5-HT<sub>1</sub> receptor antagonist in AOB MCs**  
 Representative raster plot and associated spike frequency line graph for an MC that exhibited slow-onset 5-HT inhibition that was inhibited by either: *A*, left, a non-selective 5-HT<sub>2,7</sub> receptor antagonist methysergide or *B*, left,

a more specific 5-HT<sub>2</sub> receptor antagonist mianserin. C, *left*, raster plot and associated spike frequency for an MC that exhibited rapid-onset 5-HT inhibition that was blocked by the 5-HT<sub>1</sub> receptor antagonist pindolol. A–C, *right*, bar graphs of the mean spike frequency expressed as percent of the basal firing of the control. Because the application of methysergide (noted as Methysergide-1) and mianserin (noted as Mianserin-1) elicited strong inhibitions, current injections were increased to elevate spike firing frequencies (noted as Methysergide-2 and Mianserin-2) prior to the co-application of 5-HT and the antagonists. NS = not significantly different, Wilcoxin signed-rank test,  $P > 0.05$ . A,  $n = 4$ ; B,  $n = 5$ ; C,  $n = 4$ . [Colour figure can be viewed at [wileyonlinelibrary.com](http://wileyonlinelibrary.com)]

could contribute to general plasticity in the olfactory system that is important for olfactory discrimination and learning. Alternatively, the uniform inhibitory response to 5-HT in the AOB could be preserved as an important mechanism to regulate hard-wired innate behaviours such as aggression.

Although our study of 5-HT modulation in the MOB pharmacologically focused on those MCs exhibiting excitation, we did observe a heterogeneous response to 5-HT similar to the earlier study by Hardy *et al.* (2005), and most recent studies by Kapoor *et al.* (2016) and Brunert *et al.* (2016). It is likely that 5-HT release from the raphe nuclei into the MOB modulates olfactory synaptic physiology both with a heterogeneous response of MCs as well as across multiple OB neuron targets (Brunert *et al.* 2016).

Our data demonstrating that MCs of the MOB are modulated rapidly and directly by 5-HT<sub>2A</sub> receptor activation to yield an increase in AP firing frequency is consistent with other reports that have explored activation of the raphe nuclei, ensemble modulation of MOB MCs, and changes in synaptic activity and the glomerular network in response to serotonin (Hardy *et al.* 2005; Schmidt & Strowbridge, 2014; Brill *et al.* 2016; Kapoor *et al.* 2016). The majority of our sampled MCs in the MOB (70%) were excited following bath application of 5-HT while a small population of MCs was found to be either inhibited or received a dual inhibition/excitation following 5-HT application, which could be attributed to an indirect mechanism involving lateral inhibition from other MCs receiving a stronger excitation by 5-HT (Urban & Sakmann, 2002). Additionally, recent studies demonstrate that 5-HT, delivered locally at the glomerular level that receives most of the serotonergic projections in the OB, also increases the spiking frequency of inhibitory interneurons such as periglomerular (PG) cells and short-axon cells (SACs) through the activation of the 5-HT<sub>2C</sub> receptor, promoting interglomerular inhibition and hence decreasing the activity of some MCs (Petzold *et al.* 2009; Brill *et al.* 2016).

Since the discovery of the heterogeneity of the brain 5-HT receptor in the 1980s, and then subsequent heterogeneity of the receptor subtypes soon thereafter, subtype-specific ligands for serotonin receptors have been sought to regulate their different downstream signalling cascades (Hoyer *et al.* 1994; Barnes & Sharp, 1999; Pithadia & Jain, 2009). As a whole, the agonists and

antagonists for 5-HT receptors are deemed 'semi-selective agents' that can support subtype identity along with other parallel methods such as cloning, *in situ* hybridization and structural approaches. Our pharmacological data demonstrating 5-HT-evoked excitation in MOB MCs is blocked by three different competitive ligands (mianserin, methysergide and spiperone) that antagonize 5-HT<sub>2A</sub> receptors (among others) corroborate earlier *in situ* and immunocytochemical studies of the distribution of this receptor subtype on the soma and dendrites of MOB MCs (McLean *et al.* 1995; Yuan *et al.* 2003). Recently Brill *et al.* (2016) electrophysiologically applied a different cadre of antagonists to model the dense serotonergic innervation of the MOB to synaptic contacts on MCs (5-HT<sub>2A</sub> subtype), external tufted cells (5-HT<sub>2A</sub> subtype) and SACs (5HT<sub>2C</sub> subtype) to suggest an increased excitatory drive onto glomerular interneurons due to 5HT<sub>2A</sub> subtype activation on MCs. Although there is no reported expression of subtype-specific receptors in the AOB, apart from the reported lack of 5-HT<sub>2A</sub> mRNA by McLean *et al.* (1995), we suspect expression of 5HT<sub>2C</sub> subtype receptors on granule cells (GCs) and 5HT<sub>1A/B</sub> on MCs as modelled in Fig. 9 based solely upon our pharmacological results and deduction of cross comparison of these 'semi-selective agents'. For example, mianserin has been reported to have much higher affinity at 5-HT<sub>2A</sub> and 5-HT<sub>2C</sub> receptors compared to other 5-HT receptor subtypes (Brunello *et al.* 1982; Hoyer, 1988). Because spiperone failed to block the 5-HT-evoked slow-onset inhibition in the AOB MCs (data not shown), combined with a reported lack of 5-HT<sub>2A</sub> mRNA (McLean *et al.* 1995), our AOB MC sensitivity to mianserin (Figs 7B and 8B) infers activation of the 5-HT<sub>2C</sub> receptor. Our data demonstrating block of the 5-HT-evoked rapid-onset inhibition in the AOB by a preferred 5-HT<sub>1A/B</sub> receptor antagonist (pindolol, Fig. 8C) and a broad 5-HT<sub>1A</sub> and 5-HT<sub>2A</sub> receptor antagonist (spiperone, data not shown) (Sundaram *et al.* 1992; Newman-Tancredi *et al.* 1997) infers the presence of direct activation of a 5-HT<sub>1A/B</sub> receptor subtype. This is also consistent with an earlier study that reported the expression of 5-HT<sub>1A</sub> receptor mRNA in the OB, but the study did not localize it to the main or the accessory bulb (Pompeiano *et al.* 1992). There appear to be two sources of inhibition in MCs of the AOB following bath application of 5-HT that we initially distinguished based upon kinetics of onset of the inhibition – a rapid- or a slow-onset inhibition. The slow-onset inhibition was suppressed

by GABA<sub>A</sub> and 5-HT<sub>2C</sub> receptor antagonists, suggesting a di-synaptic mechanism involving the activation of GABAergic interneurons expressing the 5-HT<sub>2C</sub> receptor. Conversely, rapid-onset inhibition by 5-HT observed in some AOB MCs was found to not respond to gabazine, but was suppressed by the ligands pindolol and spiperone that antagonize the 5-HT<sub>1A</sub> receptor. This is consistent with its observed direct inhibition in the rapid-onset class of modulation, given that the 5-HT<sub>1A</sub> receptor is coupled to Gi/Go proteins and mediates inhibitory neurotransmission (Palacios, 2016).

Beyond our discovery of a differential modulation by serotonin between the MOB and AOB, others have reported opposing effects in such parallel odour

processing pathways for neuromodulators such as noradrenaline (Nai *et al.* 2009) or acetylcholine (Smith *et al.* 2015). The opposing responses are underlined by a difference of receptor subtype expression between the MOB and the AOB and also the sensitivity of the different inhibitory interneurons to these neuromodulators in both circuits. For example, Smith *et al.* (2015) demonstrate that MCs of both systems are regulated in opposing fashion by acetylcholine, resulting in an inhibition in the MOB, and conversely an excitation in the AOB. This difference relied on the expression of the muscarinic acetylcholine receptor (mAChR) M2 in the MOB inhibiting MCs, whereas M1-mAChR expressed in the AOB directly exciting MCs. Similarly, GCs present in the AOB and MOB were found to respond differently to acetylcholine due to a different distribution of M1- and M2-mAChRs (Smith *et al.* 2015). Note that inhibition of MC output does not necessary correlate with a loss of function. Many studies have demonstrated that for both the MOB and the AOB, the response to a specific chemical stimulus triggers both activation and inhibition of MCs (Luo *et al.* 2003; Olsen & Wilson, 2008). Inhibition is essential to reduce the signal-to-noise ratio and increase the contrast of MC responses, in order to generate distinct temporal and spatial patterns of activation (Economo *et al.* 2016).

Differential neuromodulation in these parallel olfactory pathways might be inherent to their respective primary function. The main olfactory system is subject to plasticity and learning (Wilson, 2002; Luo *et al.* 2003; Mouly & Sullivan, 2010; Lepousez *et al.* 2014) while the accessory system is linked with the amygdala and hypothalamus and is specialized in the integration of semiochemical signals arising from mates or predators, triggering stereotyped innate behaviours including social interaction or danger avoidance (Dulac & Torello, 2003; Trotier, 2011; Takahashi, 2014). In the MOB, it has been suggested that 5-HT modulates the odour input by reducing the odour-evoked synaptic activity and reducing the gain of sensitivity (Petzold *et al.* 2009). However, 5-HT depletion in the OB reduces odour discrimination in rats (Moriizumi *et al.* 1994) and also impairs the olfactory learning ability of neonatal rats through a 5-HT<sub>2</sub> receptor-dependent mechanism (McLean *et al.* 1993, 1996). Interestingly, 5-HT acts in collaboration with noradrenaline in olfactory learning (Price *et al.* 1998; Yuan *et al.* 2000). It has been shown that 5-HT (through the 5-HT<sub>2A</sub> receptor) and noradrenaline (through the  $\beta$ 1-adrenoceptor) work together by co-regulating a cAMP signalling pathway in MCs in the MOB (Yuan *et al.* 2003). To our knowledge, no studies have directly explored the effect of 5-HT in the mammalian AOB. In the moth, 5-HT modulates the activity of neurons in the central lobes that receive input from olfactory sensory neurons (Kloppenburg & Mercer, 2008). Interestingly, some behavioural effects resulting from bulbectomy (increased aggression and reduced

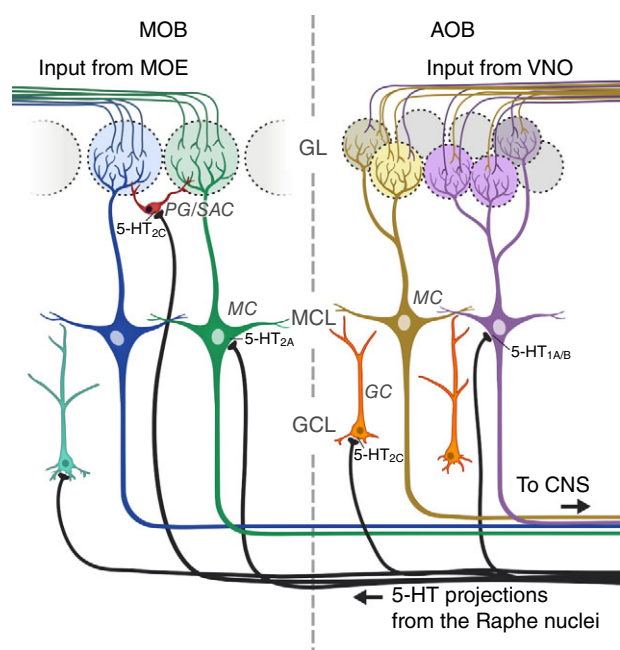


**Figure 9. Model of serotonergic modulation in two parallel processing pathways of the olfactory system**

Serotonergic (5-HT) projections from the Raphe nuclei extend to interneurons and primary projection neurons of the main (MOB) and accessory (AOB) olfactory bulbs. In the primary output neurons of each system, mitral cells can respond to 5-HT via the 5-HT<sub>2A</sub> and 5-HT<sub>1A/B</sub> receptors, respectively. Activation of 5-HT<sub>2A</sub> elicits direct excitation of MCs in the MOB and as coupled to Go/Gi signalling, activation of 5-HT<sub>1A/B</sub> evokes inhibition of MCs in the AOB. The same subclass of serotonergic receptor, 5-HT<sub>2C</sub>, is found on interneurons in both systems, but associated with different interneurons – PG/SAC in the MOB versus GC in the AOB. Note circuit differences allowing input from MOE and VNO, respectively, that could coordinate different behavioural outputs in response to 5-HT availability in each system. MOB, main olfactory bulb; MOE, main olfactory epithelium; AOB, accessory olfactory bulb; VNO, vomeronasal organ; GL, glomerular layer; MCL, mitral cell layer; GCL, granule cell layer; PG/SAC, periglomerular/short-axon cells; GC, granule cell; CNS, central nervous system. [Colour figure can be viewed at [wileyonlinelibrary.com](http://wileyonlinelibrary.com)]



sexual behaviours; Kelly *et al.* 1997) can be mimicked by injection of selective serotonergic neurotoxin 5,6- or 5,7-dihydroxytryptamine into the OB (Cairncross *et al.* 1979). Moreover, the 5-HT<sub>1</sub> receptor has been implicated in aggressive behaviours through pharmacological studies (Olivier & van Oorschot, 2005; de Boer & Koolhaas, 2005). In particular, when the 5-HT<sub>1A</sub> receptor is activated by agonists, animals show decreased aggressive behaviour (de Boer *et al.* 1999, 2000). Similarly, in teleost fish, serotonin plays a primary inhibitory role in aggressive behaviour (Munro, 1986; Winberg *et al.* 2001; Perreault *et al.* 2003).

Further functional studies are necessary to explore whether the biophysical differences we observed in serotonergic modulation across the MOB and AOB may correlate to each system's respective primary function. Having a greater knowledge base on 5-HT receptor pharmacology and changes in AP firing frequency of the major output neuron in each system provides a strong set point to design the dimensions of such behavioural studies.

## References

- Araneda S, Gamrani H, Font C, Calas A, Pujol JF & Bobillier P (1980). Retrograde axonal transport following injection of [<sup>3</sup>H]-serotonin into the olfactory bulb. II. Radioautographic study. *Brain Res* **196**, 417–427.
- Balu R, Larimer P & Strowbridge BW (2004). Phasic stimuli evoke precisely timed spikes in intermittently discharging mitral cells. *J Neurophysiol* **92**, 743–753.
- Barnes NM & Sharp T (1999). A review of central 5-HT receptors and their function. *Neuropharmacology* **38**, 1083–1152.
- Berger M, Gray JA & Roth BL (2009). The expanded biology of serotonin. *Annu Rev Med* **60**, 355–366.
- Blier P, Pineyro G, el Mansari M, Bergeron R & de Montigny C (1998). Role of somatodendritic 5-HT autoreceptors in modulating 5-HT neurotransmission. *Ann N Y Acad Sci* **861**, 204–216.
- Brill J, Shao Z, Puche AC, Wachowiak M & Shipley MT (2016). Serotonin increases synaptic activity in olfactory bulb glomeruli. *J Neurophysiol* **115**, 1208–1219.
- Broadwell RD & Jacobowitz DM (1976). Olfactory relationships of the telencephalon and diencephalon in the rabbit. III. The ipsilateral centrifugal fibers to the olfactory bulbar and retrobulbar formations. *J Comp Neurol* **170**, 321–345.
- Brunello N, Chuang DM & Costa E (1982). Different synaptic location of mianserin and imipramine binding sites. *Science* **215**, 1112–1115.
- Brunert D, Tsuno Y, Rothermel M, Shipley MT & Wachowiak M (2016). Cell-type-specific modulation of sensory responses in olfactory bulb circuits by serotonergic projections from the raphe nuclei. *J Neurosci* **36**, 6820–6835.
- Cairncross KD, Cox B, Forster C & Wren AF (1979). Olfactory projection systems, drugs and behaviour: a review. *Psychoneuroendocrinology* **4**, 253–272.
- de Boer SF & Koolhaas JM (2005). 5-HT<sub>1A</sub> and 5-HT<sub>1B</sub> receptor agonists and aggression: a pharmacological challenge of the serotonin deficiency hypothesis. *Eur J Pharmacol* **526**, 125–139.
- de Boer SF, Lesourd M, Mocaer E & Koolhaas JM (1999). Selective antiaggressive effects of alnespirone in resident-intruder test are mediated via 5-hydroxytryptamine<sub>1A</sub> receptors: a comparative pharmacological study with 8-hydroxy-2-dipropylaminotetralin, ipsapirone, buspirone, eltoprazine, and WAY-100635. *J Pharmacol Exp Ther* **288**, 1125–1133.
- de Boer SF, Lesourd M, Mocaer E & Koolhaas JM (2000). Somatodendritic 5-HT<sub>1A</sub> autoreceptors mediate the anti-aggressive actions of 5-HT<sub>1A</sub> receptor agonists in rats: an ethopharmacological study with S-15535, alnespirone, and WAY-100635. *Neuropsychopharmacology* **23**, 20–33.
- de Olmos J, Hardy H & Heimer L (1978). The afferent connections of the main and the accessory olfactory bulb formations in the rat: an experimental HRP-study. *J Comp Neurol* **181**, 213–244.
- Devore S & Linster C (2012). Noradrenergic and cholinergic modulation of olfactory bulb sensory processing. *Front Behav Neurosci* **6**, 52.
- Diuzhikova NA, Pavlova MB & Novikov SN (1987). [Serotonin level in the olfactory bulbs and pheromone-mediated regulation of aggressive behavior in male domestic mice]. *Dokl Akad Nauk SSSR* **292**, 1275–1277.
- Dulac C & Torello AT (2003). Molecular detection of pheromone signals in mammals: from genes to behaviour. *Nat Rev Neurosci* **4**, 551–562.
- Economu MN, Hansen KR & Wachowiak M (2016). Control of mitral/tufted cell output by selective inhibition among olfactory bulb glomeruli. *Neuron* **91**, 397–411.
- Fadool DA, Tucker K & Pedarzani P (2011). Mitral cells of the olfactory bulb perform metabolic sensing and are disrupted by obesity at the level of the Kv1.3 ion channel. *PLoS One* **6**, e24921.
- Figueres-Onate M, Gutierrez Y & Lopez-Mascaraque L (2014). Unraveling Cajal's view of the olfactory system. *Front Neuroanat* **8**, 55.
- Grundy D (2015). Principles and standards for reporting animal experiments in *The Journal of Physiology* and *Experimental Physiology*. *J Physiol* **593**, 2547–2549.
- Hardy A, Palouzier-Paulignan B, Duchamp A, Royet JP & Duchamp-Viret P (2005). 5-Hydroxytryptamine action in the rat olfactory bulb: in vitro electrophysiological patch-clamp recordings of juxtglomerular and mitral cells. *Neuroscience* **131**, 717–731.
- Hovis KR, Ramnath R, Dahlen JE, Romanova AL, LaRocca G, Bier ME & Urban NN (2012). Activity regulates functional connectivity from the vomeronasal organ to the accessory olfactory bulb. *J Neurosci* **32**, 7907–7916.
- Hoyer D (1988). Functional correlates of serotonin 5-HT<sub>1</sub> recognition sites. *J Recept Res* **8**, 59–81.
- Hoyer D, Clarke DE, Fozard JR, Hartig PR, Martin GR, Mylecharane EJ, Saxena PR & Humphrey PP (1994). International Union of Pharmacology classification of receptors for 5-hydroxytryptamine (serotonin). *Pharmacol Rev* **46**, 157–203.

- Jacobs BL & Azmitia EC (1992). Structure and function of the brain serotonin system. *Physiol Rev* **72**, 165–229.
- Jia C, Chen WR & Shepherd GM (1999). Synaptic organization and neurotransmitters in the rat accessory olfactory bulb. *J Neurophysiol* **81**, 345–355.
- Kapoor V, Provost AC, Agarwal P & Murthy VN (2016). Activation of raphe nuclei triggers rapid and distinct effects on parallel olfactory bulb output channels. *Nat Neurosci* **19**, 271–282.
- Kelly JP, Wrynn AS & Leonard BE (1997). The olfactory bulbectomized rat as a model of depression: an update. *Pharmacol Ther* **74**, 299–316.
- Kloppenburg P & Mercer AR (2008). Serotonin modulation of moth central olfactory neurons. *Annu Rev Entomol* **53**, 179–190.
- Krimer LS & Goldman-Rakic PS (1997). An interface holding chamber for anatomical and physiological studies of living brain slices. *J Neurosci Methods* **75**, 55–58.
- Larriva-Sahd J (2008). The accessory olfactory bulb in the adult rat: a cytological study of its cell types, neuropil, neuronal modules, and interactions with the main olfactory system. *J Comp Neurol* **510**, 309–350.
- Lepousez G, Nissant A, Bryant AK, Gheusi G, Greer CA & Lledo PM (2014). Olfactory learning promotes input-specific synaptic plasticity in adult-born neurons. *Proc Natl Acad Sci USA* **111**, 13984–13989.
- Liu S, Aungst JL, Puche AC & Shipley MT (2012). Serotonin modulates the population activity profile of olfactory bulb external tufted cells. *J Neurophysiol* **107**, 473–483.
- Luo M, Fee MS & Katz LC (2003). Encoding phomonal signals in the accessory olfactory bulb of behaving mice. *Science* **299**, 1196–1201.
- McLean JH, Darby-King A & Hodge E (1996). 5-HT<sub>2</sub> receptor involvement in conditioned olfactory learning in the neonate rat pup. *Behav Neurosci* **110**, 1426–1434.
- McLean JH, Darby-King A & Paterno GD (1995). Localization of 5-HT<sub>2A</sub> receptor mRNA by in situ hybridization in the olfactory bulb of the postnatal rat. *J Comp Neurol* **353**, 371–378.
- McLean JH, Darby-King A, Sullivan RM & King SR (1993). Serotonergic influence on olfactory learning in the neonate rat. *Behav Neural Biol* **60**, 152–162.
- McLean JH & Shipley MT (1987). Serotonergic afferents to the rat olfactory bulb: I. Origins and laminar specificity of serotonergic inputs in the adult rat. *J Neurosci* **7**, 3016–3028.
- Millan MJ, Marin P, Bockaert J & Mannoury la CC (2008). Signaling at G-protein-coupled serotonin receptors: recent advances and future research directions. *Trends Pharmacol Sci* **29**, 454–464.
- Mittal R, Debs LH, Patel AP, Nguyen D, Patel K, O'Connor G, Grati M, Mittal J, Yan D, Eshraghi AA, Deo SK, Daunert S & Liu XZ (2016). Neurotransmitters: The critical modulators regulating gut-brain axis. *J Cell Physiol*. DOI: 10.1002/jcp.25518.
- Moriizumi T, Tsukatani T, Sakashita H & Miwa T (1994). Olfactory disturbance induced by deafferentation of serotonergic fibers in the olfactory bulb. *Neuroscience* **61**, 733–738.
- Morikawa H, Manzoni OJ, Crabbe JC & Williams JT (2000). Regulation of central synaptic transmission by 5-HT<sub>1B</sub> auto- and heteroreceptors. *Mol Pharmacol* **58**, 1271–1278.
- Mouly AM & Sullivan R (2010). Memory and plasticity in the olfactory system: from infancy to adulthood. In Menini A, ed. *The Neurobiology of Olfaction*. Chapter 15. CRC Press/Taylor and Francis, Boca Raton, FL.
- Munro AD (1986). Effects of melatonin, serotonin, and naloxone on aggression in isolated cichlid fish (*Aequidens pulcher*). *J Pineal Res* **3**, 257–262.
- Nai Q, Dong HW, Hayar A, Linster C & Ennis M (2009). Noradrenergic regulation of GABAergic inhibition of main olfactory bulb mitral cells varies as a function of concentration and receptor subtype. *J Neurophysiol* **101**, 2472–2484.
- Newman-Tancredi A, Conte C, Chaput C, Spedding M & Millan MJ (1997). Inhibition of the constitutive activity of human 5-HT<sub>1A</sub> receptors by the inverse agonist, spiperone but not the neutral antagonist, WAY 100,635. *Br J Pharmacol* **120**, 737–739.
- Noguchi T, Sasajima H, Miyazono S & Kashiwayanagi M (2014). Similar rate of information transfer on stimulus intensity in accessory and main olfactory bulb output neurons. *Neurosci Lett* **576**, 56–61.
- Ogren SO, Eriksson TM, Elvander-Tottie E, D'Addario C, Ekstrom JC, Svenningsson P, Meister B, Kehr J & Stiedl O (2008). The role of 5-HT<sub>(1A)</sub> receptors in learning and memory. *Behav Brain Res* **195**, 54–77.
- Olivier B & van Oorschot R (2005). 5-HT<sub>1B</sub> receptors and aggression: a review. *Eur J Pharmacol* **526**, 207–217.
- Olsen SR & Wilson RI (2008). Lateral presynaptic inhibition mediates gain control in an olfactory circuit. *Nature* **452**, 956–960.
- Palacios JM (2016). Serotonin receptors in brain revisited. *Brain Res* **1645**, 46–49.
- Perreault HA, Semsar K & Godwin J (2003). Fluoxetine treatment decreases territorial aggression in a coral reef fish. *Physiol Behav* **79**, 719–724.
- Petzold GC, Hagiwara A & Murthy VN (2009). Serotonergic modulation of odor input to the mammalian olfactory bulb. *Nat Neurosci* **12**, 784–791.
- Pithadia AB & Jain SM (2009). 5-Hydroxytryptamine receptor subtypes and their modulators with therapeutic potentials. *J Clin Med Res* **1**, 72–80.
- Pompeiano M, Palacios JM & Mengod G (1992). Distribution and cellular localization of mRNA coding for 5-HT<sub>1A</sub> receptor in the rat brain: correlation with receptor binding. *J Neurosci* **12**, 440–453.
- Price TL, Darby-King A, Harley CW & McLean JH (1998). Serotonin plays a permissive role in conditioned olfactory learning induced by norepinephrine in the neonate rat. *Behav Neurosci* **112**, 1430–1437.
- Ramon y Cajal (1911). *Histologie du système nerveux de l'homme et des vertébrés*. Maloine, Paris.
- Reynolds GP, Templeman LA & Zhang ZJ (2005). The role of 5-HT<sub>2C</sub> receptor polymorphisms in the pharmacogenetics of antipsychotic drug treatment. *Prog Neuropsychopharmacol Biol Psychiatry* **29**, 1021–1028.
- Roth BL (1994). Multiple serotonin receptors: clinical and experimental aspects. *Ann Clin Psychiatry* **6**, 67–78.

- Roth BL (2007). The serotonin receptors: from molecular pharmacology to human therapeutics. In *Chemical Neuroanatomy of 5-HT Receptor Subtypes in the Mammalian Brain*, eds Mengod G, Vilaro MT, Cortes R, Lopez-Gimenez JF, Raurich A & Palacios JM, pp. 319–364. Humana Press, Totowa, NJ.
- Roth BL & Xia Z (2004). Molecular and cellular mechanisms for the polarized sorting of serotonin receptors: relevance for genesis and treatment of psychosis. *Crit Rev Neurobiol* **16**, 229–236.
- Salazar I, Sanchez QP, Lombardero M & Cifuentes JM (2001). Histochemical identification of carbohydrate moieties in the accessory olfactory bulb of the mouse using a panel of lectins. *Chem Senses* **26**, 645–652.
- Schmidt LJ & Strowbridge BW (2014). Modulation of olfactory bulb network activity by serotonin: synchronous inhibition of mitral cells mediated by spatially localized GABAergic microcircuits. *Learn Mem* **21**, 406–416.
- Shpak G, Zylbertal A, Yarom Y & Wagner S (2012). Calcium-activated sustained firing responses distinguish accessory from main olfactory bulb mitral cells. *J Neurosci* **32**, 6251–6262.
- Smith RS, Hu R, DeSouza A, Eberly CL, Krahe K, Chan W & Araneda RC (2015). Differential muscarinic modulation in the olfactory bulb. *J Neurosci* **35**, 10773–10785.
- Steel RGD & Torrie JH (1980). *Principles and Procedures of Statistics: A Biometrical Approach*. McGraw Hill, New York, NY.
- Sundaram H, Newman-Tancredi A & Strange PG (1992). Pharmacological characterisation of the 5-HT<sub>1A</sub> serotonin receptor using the agonist [<sup>3</sup>H]8-OH-DPAT, and the antagonist [<sup>3</sup>H]spiperone. *Biochem Soc Trans* **20**, 145S.
- Suzuki Y, Kiyokage E, Sohn J, Hioki H & Toida K (2015). Structural basis for serotonergic regulation of neural circuits in the mouse olfactory bulb. *J Comp Neurol* **523**, 262–280.
- Takahashi LK (2014). Olfactory systems and neural circuits that modulate predator odor fear. *Front Behav Neurosci* **8**, 72.
- Takami S & Graziadei PP (1990). Morphological complexity of the glomerulus in the rat accessory olfactory bulb—a Golgi study. *Brain Res* **510**, 339–342.
- Takeuchi Y, Kimura H & Sano Y (1982). Immunohistochemical demonstration of serotonin nerve fibers in the olfactory bulb of the rat, cat and monkey. *Histochemistry* **75**, 461–471.
- Trotier D (2011). Vomeronasal organ and human pheromones. *Eur Ann Otorhinolaryngol Head Neck Dis* **128**, 184–190.
- Urban NN & Castro JB (2005). Tuft calcium spikes in accessory olfactory bulb mitral cells. *J Neurosci* **25**, 5024–5028.
- Urban NN & Sakmann B (2002). Reciprocal intraglomerular excitation and intra- and interglomerular lateral inhibition between mouse olfactory bulb mitral cells. *J Physiol* **542**, 355–367.
- Vergnes M, Mack G & Kempf E (1974). [Inhibitory control of mouse-killing behaviour in the rat: serotonergic system of the raphe and olfactory input (author's transl)]. *Brain Res* **70**, 481–491.
- Wilson CS (2002). Reasons for eating: personal experiences in nutrition and anthropology. *Appetite* **38**, 63–67.
- Winberg S, Overli O & Lepage O (2001). Suppression of aggression in rainbow trout (*Oncorhynchus mykiss*) by dietary L-tryptophan. *J Exp Biol* **204**, 3867–3876.
- Yuan Q, Harley CW, Bruce JC, Darby-King A & McLean JH (2000). Isoproterenol increases CREB phosphorylation and olfactory nerve-evoked potentials in normal and 5-HT-depleted olfactory bulbs in rat pups only at doses that produce odor preference learning. *Learn Mem* **7**, 413–421.
- Yuan Q, Harley CW & McLean JH (2003). Mitral cell beta1 and 5-HT<sub>2A</sub> receptor colocalization and cAMP coregulation: a new model of norepinephrine-induced learning in the olfactory bulb. *Learn Mem* **10**, 5–15.
- Zibman S, Shpak G & Wagner S (2011). Distinct intrinsic membrane properties determine differential information processing between main and accessory olfactory bulb mitral cells. *Neuroscience* **189**, 51–67.

## Additional information

### Conflicts of interest

The authors declare that they have no competing interests.

### Author contributions

ZH was responsible for the collection of all electrophysiological data. All authors designed the experiments, assembled and interpreted the data, aided in spike analysis, and wrote the manuscript.

### Funding

This work was supported by the National Institutes of Health (NIH) R01 DC013080 from the National Institutes of Deafness and Communication Disorders (NIDCD).

### Acknowledgements

We would like to thank J. Anthony Warrington, Wesley Joshua Earl and Abigail Thomas for routine technical assistance and mouse husbandry. We would like to thank Mr. Charles Badland for graphical assistance in Figure 9.